

Surface Waves Induced by a Moving Submarine Model

Linjie Li¹, Binbin Zhao¹ and Baikang Sun¹

Received: 24 September 2022 / Accepted: 12 December 2022
© Harbin Engineering University and Springer-Verlag GmbH Germany, part of Springer Nature 2023

Abstract

A moving submarine can generate internal waves, as well as extremely small free surface waves, in a fluid with density stratification. In this study, the internal and free surface wave wakes caused by a moving submarine in two layers of constant density fluid were studied numerically using the commercial software STAR-CCM+. The realizable $k-\varepsilon$ turbulence model was used to solve the Reynolds-averaged Navier–Stokes equation, and the volume of the fluid method was used to monitor the fluctuations of the internal interface and free surface. Different cases of a moving submarine with different cruising speeds and relative diving depths were studied. Results showed that the maximum fluctuation amplitude of the free surface increased as the speed of the submarine increased; however, the maximum fluctuation amplitude of the internal interface first decreased and then increased. When the submarine moved at the maximum cruising speed, the maximum fluctuation amplitude of the free surface decreased as the diving depth increased, while the wavelength of the free surface wave was basically the same. If the submarine moved at the minimum cruising speed, then the wave elevation in the free surface was extremely small, but the internal surface had obviously large-amplitude internal waves, and the relative diving depth had a great influence on internal waves.

Keywords Free surface wave; Internal wave; Submarine; Density stratification; Cruising speed; Relative diving depth

1 Introduction

The ocean, especially the South China Sea, is characterized by density stratification because of the influence of temperature differences, salinity, and other factors (Zhang et al. 2006; Liu et al. 2013). Underwater objects moving in a stratified liquid will generate a wake at the inner interface and free surface.

Some research has been conducted regarding density-stratified flow. Landau and Lifshitz (1959) provided the dispersion relation of the interface between two layers of

fluid under the assumption of a rigid lid. Grue et al. (1997) studied the problem of large internal solitary waves excited by a semi-elliptical object moving on the seabed at a 4:1 thickness ratio and 0.787 density ratio of the upper and lower liquids. Wang et al. (2022) studied the influence of different internal wave environments on the hydrodynamic characteristics of vehicles. The above studies regarded the free surface as a rigid lid to simplify the problem.

Some researchers preserved the free surface in their work. Yeung and Nuyen (1999) proposed that waves generated by a moving source in a two-layer ocean of finite depth should have surface and internal wave modes. Wei et al. (2003) studied the surface effects of internal waves generated by a moving source in a two-layer fluid with finite depth. Faltinsen (2006) proposed that if the density Froude number corresponding to an object's speed was greater than 1, then the interface will contain only divergent waves, and if the density Froude number was less than 1, then the interface can exist simultaneously with the transverse and divergent waves. Zhao et al. (2022) extended the Miyata–Choi–Camassa free surface model to bottom-time-varying problems. However, these theories do not consider the viscosity of the liquid.

With the development of computing analysis, researchers

Article Highlights

- This study numerically validated the free surface and internal wave results of Liu et al. (2021a);
- The influence of submarine cruising speed on free surface waves was studied;
- The influence of relative diving depth on internal surface waves was studied when a submarine moved at the minimum cruising speed.

✉ Binbin Zhao
zhaobinbin@hrbeu.edu.cn

¹ College of Shipbuilding Engineering, Harbin Engineering University, Harbin 150001, China

have begun to perform numerical simulations of stratified fluids. Luo et al. (2007), Ding et al. (2016), Li et al. (2018), Ma et al. (2020), Liu et al. (2020, 2021a), and He et al. (2022) studied the surface waves and internal wave wake caused by the movement of a submarine, but their results were not validated. He et al. (2021), Liu et al. (2021c) and Dong et al. (2022) studied the effect of density stratification on the wave-making resistance of submarines. The influence of appendages on the hydrodynamic characteristics of submarines in stratified flow was studied by Liu et al. (2021b). In addition to a two-layer fluid system, Hu et al. (2020) and Huang et al. (2020, 2022) studied the wake excited by submarine motion under the condition of continuous density change. Yu and Hu (2022) studied the effect of acceleration and deceleration of a submarine on wake characteristics in the case where the submarine's motion is time-invariant.

In the above numerical simulation studies, the corresponding real-scale submarine speeds are all greater than 10 kn. However, detecting surface waves is easier as the speed of the submarine increases. Yet considering the situation where a submarine cruises at low speeds, such as 4 kn, is still worthwhile.

The motivation of this work was to study the surface waves induced by a moving submarine and to numerically validate the results of other free surface and internal waves. The remainder of this paper is organized as follows. In the second section, the numerical model is introduced. In the third section, the numerical results and analysis are presented. In the fourth section, the conclusions are listed.

2 Numerical calculation model

This study considers the free surface and internal surface wake of the SUBOFF fully attached submarine in a strongly stratified liquid. The thickness of the upper fluid h_1 is small, and the density of the liquid is ρ_1 , while the thickness of the lower fluid h_2 is larger, and the density of the liquid is ρ_2 . The submarine has a steady motion at different depths and speeds, and its motion disturbs the free surface and interface to form a wake. A layer of air was added above the upper liquid, as shown in Figure 1 (taking the submarine in the lower liquid as an example), to study the free surface wake.

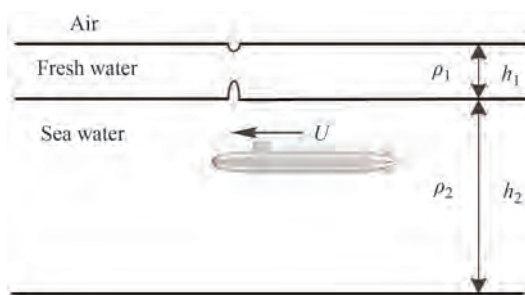


Figure 1 Diagram of the computational domain

2.1 Governing equation

The mass and momentum conservation equations (i.e., the Navier–Stokes [N-S] equation) satisfied by the flow mass point in the STAR-CCM + solution are as follows:

$$\frac{\partial \rho}{\partial t} + \nabla \cdot \rho \mathbf{v} = 0 \quad (1)$$

$$\rho \frac{D\mathbf{v}}{Dt} = \rho \mathbf{g} - \nabla p + \mu \nabla^2 \mathbf{v} \quad (2)$$

where ρ is the density of the fluid in each layer, \mathbf{v} is the velocity of the fluid particle, p is the pressure, and $g=9.81 \text{ m/s}^2$ is the gravitational acceleration. The Reynolds-averaged N-S (RANS) equation can be obtained by a time-uniformizing N-S equation, and then the RANS equation can be solved using the realizable k - ε turbulence model.

2.2 Capturing the internal interface with the VOF method

The internal wave interface was tracked and solved using the volume of fluid (VOF) method. This method solves the interface problems by calculating the volume fraction of each phase in each grid; the VOF is also widely used in the finite volume method at present (Denner and Wachem 2014).

Assuming $r^{(k)}$ is the proportion of the k th phase in a cell grid according to the conservation of mass, we obtain

$$\sum_{k=1}^n r^{(k)} = 1 \quad (3)$$

The volume fraction $r^{(k)}$ can be determined from the ratio of the volume of each phase to the total volume as follows:

$$r^{(k)} = \frac{V^{(k)}}{\sum_{k=1}^n V^{(k)}} \quad (4)$$

In this study, because the free surface is reserved, three phases exist, namely, air, fresh water, and sea water. Thus, $n = 3$ and $k = 1, 2$, and 3 . The fluctuation of the free surface and internal wave interface can be determined by monitoring the vertical position of the isosurface, each with a 50% volume fraction of air and water.

2.3 Boundary conditions

The submarine surface is set as the no-slip wall boundary; the inlet, top, bottom, and side are set as the velocity inlet boundary condition, and the outlet is set as the free-flow outlet boundary condition, as shown in Figure 2 (taking the submarine below the internal interface as an example).

The densities of air, fresh water, and sea water are defined

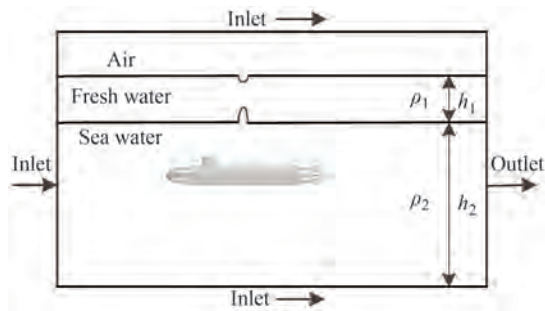


Figure 2 Schematic of the boundary condition setting

by the Euler multiphase flow model, and the initial distribution of each phase and the pressure function are set by a user-defined field function module.

3 Results and analysis

The numerical results of this study were compared and verified using the example of Liu et al. (2021a). Then, the effects of submarine cruising speed and relative diving depth were studied.

3.1 Solution validation

For the two-layer fluid system with a constant density, Liu et al. (2021a) studied the wave generation problem of submarine motion in the upper fluid based on the model of the SUBOFF fully attached submarine. The geometric model is shown in Figure 3, and the principal dimensions are given in Table 1. The upper surface of the upper fluid retained the free surface. The length of the SUBOFF fully attached submarine model is $L = 3$ m, the thickness of the upper fluid is $h_1 = 0.24L = 0.72$ m, and the density is $\rho_1 = 997.561$ kg/m³; the thickness of the lower fluid is $h_2 = 2$ m, and the density is $\rho_2 = 1020$ kg/m³; and the thickness ratio of the upper and



Figure 3 SUBOFF geometric model

Table 1 Main parameters of the SUBOFF model

Parameters	Symbol	Full scale	Model
Scale	λ	1	33.133
Length	L (m)	99.4	3
Maximum diameter	D_{\max} (m)	11.6	0.348
Longitudinal center on buoyancy	X_B (m)	45.9	1.386
Wetted surface area	S_{wa} (m ²)	3123.2	2.845

lower layers is $h_1/h_2 = 0.36$, and the density ratio is $\rho_1/\rho_2 = 0.978$. The submarine moves in the upper liquid at a constant velocity of $U = 2.712$ m/s, and the submarine's center of gravity is $d_1 = 0.12L = 0.36$ m above the internal interface. The motion of the submarine disturbs the interface and generates the wake of the wave (Figure 4).

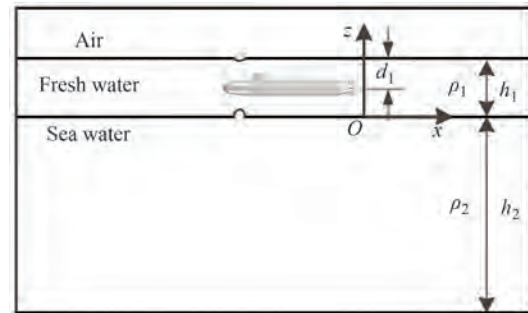


Figure 4 Schematic representation of a submarine moving above the internal interface

Trimmed meshes and prism layer meshes were generated in STAR-CCM+. More cells were added in the zone near the SUBOFF model and the associative zone from the free surface to the internal interface to ensure the proper resolution. A slow volume growth rate was set. The grid refinement is shown in Figure 5, with a total of 23 million cells. The grid size of each region is detailed in Table 2. During the simulation, the time step was set as $\Delta t = 0.01$ s, and the maximum number of inner iterations was 10.

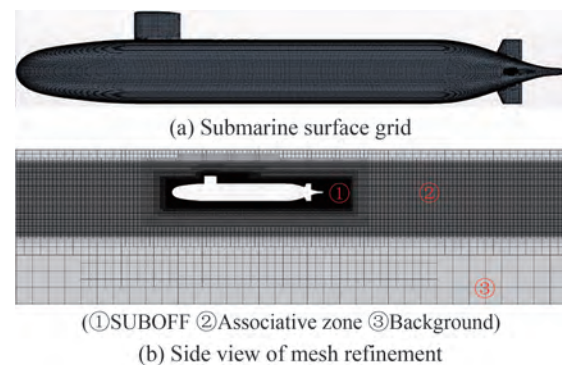


Figure 5 Mesh refinement of the domain

Table 2 Grid refinement of each region

Block name	No.	Mesh size (dx, dy, dz)		
SUBOFF	1	$L/600$	$L/600$	$L/600$
Associative zone	2	$L/37.5$	$L/37.5$	$L/600$
Background	3	$L/9.375$	$L/9.375$	$L/9.375$

To verify the reliability of the numerical model used in this study, a numerical simulation was performed to reproduce the calculation example of Liu et al. (2021a). The nu-

merical calculation results in this study were compared with the free surface and internal interface wave heights reported in the literature, as shown in Figure 6 (obtained from the tangent between the longitudinal section in the submarine and the internal interface).

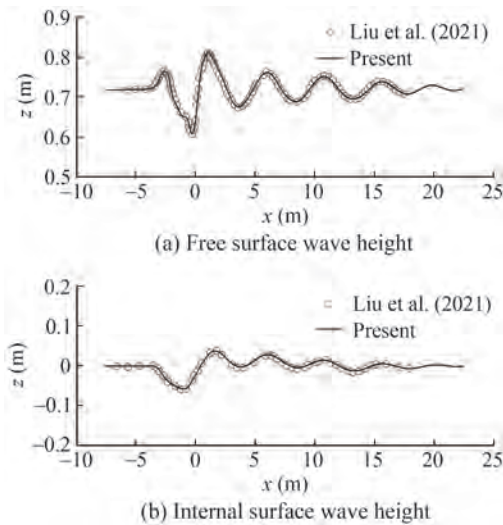


Figure 6 Wave heights of free surface and internal interface

As can be seen from Figure 6, the internal wave results of submarine motion excitation in the layered flow obtained by STAR-CCM+ in this study coincide with the results of Liu et al. (2021a), thus verifying the accuracy of the present study's numerical results.

3.2 Influence of submarine cruising speed

The speed of the submarine model considered in Section 3.1 corresponds to the speed of the real-scale submarine, which is 30.4 kn, but the cruising speed of the real-scale submarine could be 4 kn. Therefore, the other parameters in Section 3.1 were kept unchanged, and only the movement velocity of the submarine was set as 4, 8, and 15 kn. The corresponding speed of the submarine model is listed in Table 3.

Table 3 Working conditions of different cruising speeds

SUBOFF	Speed			
Model (3 m)	2.712 m/s	1.341 m/s	0.714 9 m/s	0.357 5 m/s
Full scale (99.4 m)	30.4 kn	15 kn	8 kn	4 kn

In this study, the SUBOFF model with $L = 3$ m was used for calculation.

The wave-making images of the free surface at four different speeds are shown in Figure 7, and the wave heights of the free surface at the different speeds are shown in Figure 8. The coordinate system is set according to Figure 4. Therefore, the equilibrium position of the still water surface is $Z_0 = 0.72$ m.

As can be seen from Figure 7, when the submarine cruises at a high speed of 2.712 m/s (equal to 30.4 kn of the real-scale model), the free surface has obvious Kelvin waves. However, as the speed becomes 1.341 m/s (equal to 15 kn of the real-scale model), the Kelvin waves are not as clear. As the

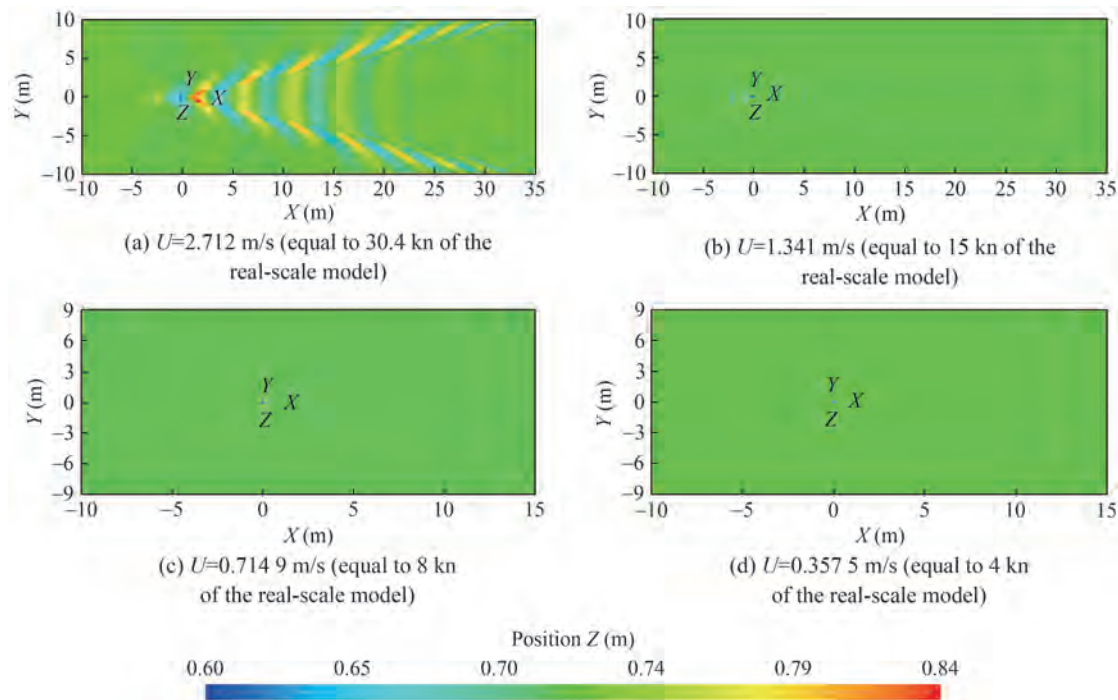


Figure 7 Top view of the free surface at different cruising speeds

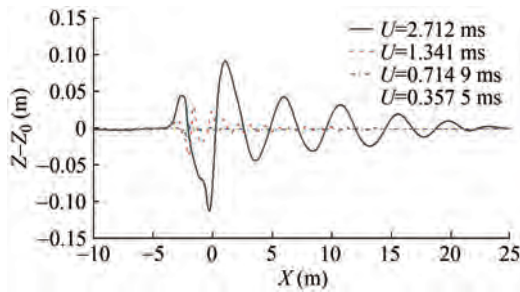


Figure 8 Free surface fluctuation of different cruising speeds at the x - z slice

velocity decreases, such as $U = 0.7149$ m/s (equal to 8 kn of the real-scale model) and $U = 0.3575$ m/s (equal to 4 kn of the real-scale model), the free surface is almost at rest.

Figure 8 indicates that the free surface fluctuation is visible only when the speed of the submarine is 2.712 and 1.341 m/s. As the speed of the submarine decreases, the maximum fluctuation of the free surface decreases significantly. For example, when the speed of the submarine decreases from 2.712 m/s to 1.341 m/s, the maximum fluctuation of the free surface is reduced by 66.89%. As the velocity continues to decrease, the maximum fluctuation of the free surface becomes negligible compared with the maximum fluctuation at 2.712 m/s.

Wave-making images of the internal surface at four different speeds are shown in Figure 9, and the wave heights of the internal surface at different speeds are shown in Figure 10. The equilibrium position of the still internal surface is $Z = 0$.

The V-shaped divergent wake is visible on the internal surface waveform at four different cruising speeds in Figure 9,

and the angle of the divergent wave increases as the speed decreases. However, transverse waves appear on the internal surface only when the speed is 2.712 m/s (equal to 30.4 kn of the real-scale model).

Figure 10 shows that the maximal fluctuation amplitude of the internal surface is 0.1026 m. However, this amplitude also occurs in the case of the lowest velocity, which is 0.3575 m/s (equal to 4 kn of the real-scale model). As the submarine velocity increases from 0.3575 m/s to 1.341 m/s, the fluctuation amplitude of the internal surface becomes small; however, the amplitude increases when the speed increases from 1.341 m/s to 2.712 m/s.

3.3 Influence of submarine relative diving depth

The cruising speed range of the real-scale submarine is 4–30 kn. Therefore, this section discusses the effect of the SUBOFF model's relative diving depth on the surface signatures at 2.712 and 0.3575 m/s. Three typically relative diving positions of the submarine were considered: above the internal surface (corresponding to d_1), on the internal surface (corresponding to d_2), and below the internal surface (corresponding to d_3). Table 2 shows the specific parameters, where d_i is the distance from the center of the submarine to the free surface.

The wave-making images of the free surface at three diving depths and at a submarine model speed of 2.712 m/s are shown in Figure 11, and the wave heights of the free surface at the different diving depths are shown in Figure 12. The equilibrium position of the still water surface was $Z_0 = 0.72$ m.

Figure 11 shows that when the submarine cruises at a high

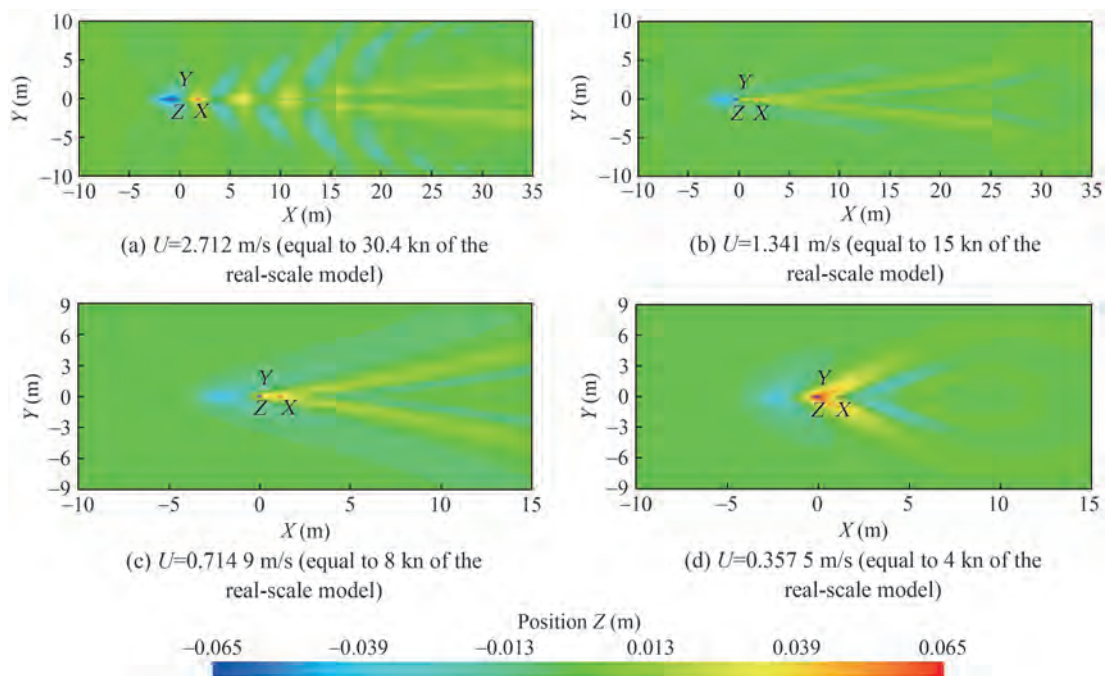


Figure 9 Top view of the internal surface at different cruising speeds

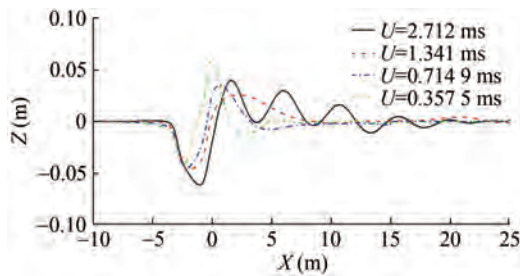


Figure 10 Internal surface fluctuation of different cruising speeds at the x - z slice

Table 4 Working conditions at different relative diving depths

Cases	d_1	d_2	d_3
d_i/L	0.12	0.24	0.36

speed of 2.712 m/s (equal to 30.4 kn of the real-scale model), the free surface always has obvious Kelvin waves regardless of the diving position. In Figure 12, the maximum fluctuation of the free surface is 0.2043 m, which occurs when the submarine is 0.12 L away from the free surface; with the distance doubled (corresponding to d_2), the maximum fluctuation is reduced by 58.2%. If the distance increases by three times (corresponding to d_3), then the maximum fluctuation is reduced by 73.3%, but the wavelength of the free surface wave is basically the same.

At a low-speed submarine model (0.357 5 m/s), the free surface had a small wave elevation, but the internal surface wave elevation was relatively large. Thus, the remain-

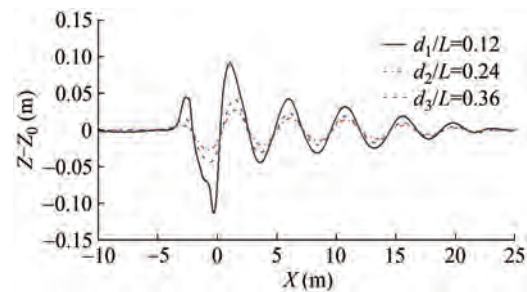


Figure 12 Free surface fluctuation of different relative diving depths at the x - z slice with high speed

der of this section considers the internal surface wave elevation when the submarine model was in different fluid layers. The top view of the internal surface wave-making images at different relative diving depths with low speed is shown in Figure 13, and the wave heights of the internal surface at different diving depths are shown in Figure 14.

A notable feature in Figure 13 is that the wave crest was in front of the wave trough when the submarine moved below the internal interface (corresponding to d_3). In contrast, this position was reversed in the other two cases (corresponding to d_1 and d_2). Another phenomenon is that when the submarine model moved on the internal surface (corresponding to d_2), the wake on the internal surface was not obvious compared with that in the other two cases (d_1 and d_3).

Figure 14 shows that even though the relative distance from the center of the submarine to the internal surface is the same (d_1 and d_3) when the submarine moves above the

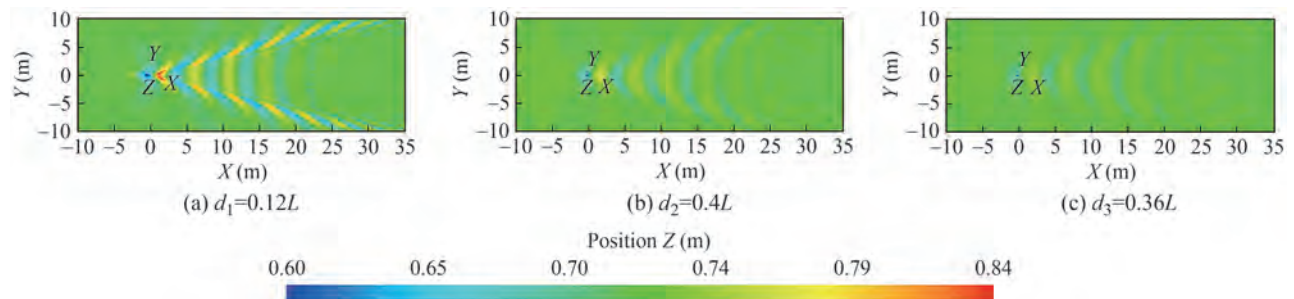


Figure 11 Top view of the free surface at different relative diving depths with high speed

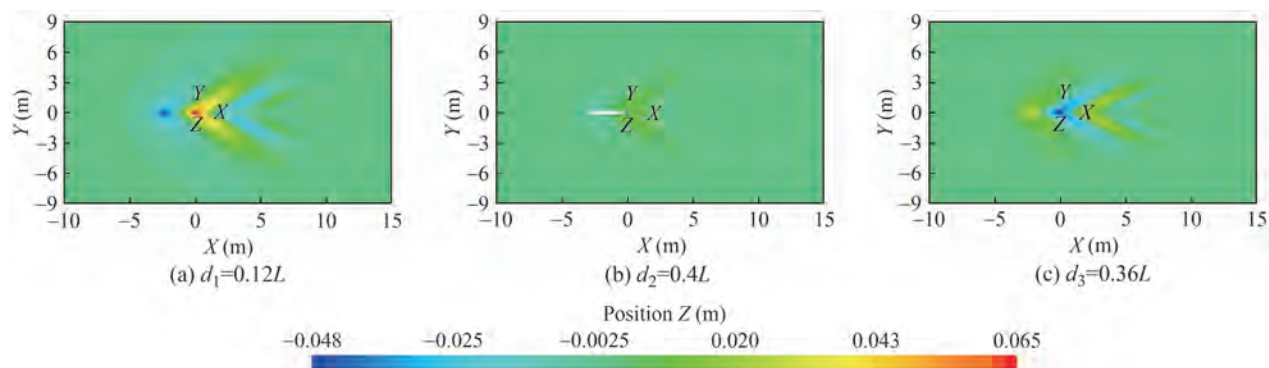


Figure 13 Top view of the internal surface at different relative diving depths with low speed

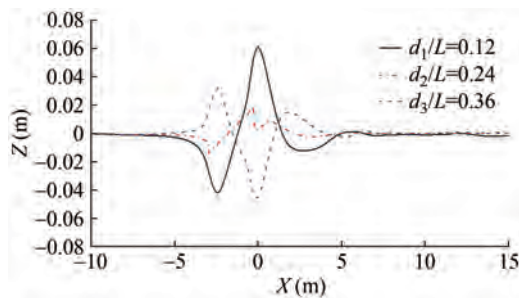


Figure 14 Internal surface fluctuation of different relative diving depths at the x - z slice with low speed

inner interface (d_1), the internal surface fluctuation amplitude is larger than that of the submarine moving below the internal interface (d_3), and the smallest amplitude appears when the submarine moves on the internal interface (d_2).

4 Conclusions

In this study, the waves of free surface and internal surface induced by a moving submarine were simulated using STAR-CCM+ commercial software, and the influence of submarine velocity and diving depth on surface waves was analyzed. The main conclusions are as follows:

1) When the submarine moved at high speed above the internal interface, the free surface and internal interface wave results were validated numerically in accordance with Liu et al. (2021a).

2) As the cruising speed of the submarine model decreased from 2.712 m/s to 0.357 5 m/s (equal to 30.4 and 4 kn, respectively, of the real-scale model), the maximum fluctuation amplitude of the free surface decreased sharply, but the maximum fluctuation amplitude of the internal surface first decreased and then increased. The internal surface fluctuation amplitude at a speed of 0.357 5 m/s can be larger than that at a speed of 2.712 m/s.

3) When the submarine model moved at the maximum cruising speed, such as 2.712 m/s (equal to 30.4 kn of the real-scale model), the maximum fluctuation amplitude of the free surface decreased as the submarine moved further away from the free surface, but the wavelength of the free surface wave was basically the same.

4) If the submarine model moved at the minimum cruising speed, such as 0.357 5 m/s (equal to 4 kn of the real-scale model), and the relative distance from the center of the submarine to the internal surface was the same, when the submarine moved above the internal interface, the internal surface fluctuation amplitude was larger than that of the submarine moving below the internal surface. When the submarine moved on the internal surface, the amplitude of the internal waves was smaller than that in the other two relative diving positions.

Funding Supported by the Frontier Science Center for Extreme Marine Environmental Fluctuation Fields; Heilongjiang Touyan Innovation Team Program.

References

- Denner F, Wachem B (2014) Compressive vof method with skewness correction to capture sharp interfaces on arbitrary meshes. *Journal of Computational Physics* 279: 127-144. DOI: 10.1016/j.jcp.2014.09.002
- Ding Y, Duan F, Han PP, Niu MC (2016) Research on the relationship between moving patterns of submerged body and the features of induced internal waves in two layer fluid. *Journal of Ship Mechanics* 20(5): 523-529. (in Chinese) DOI: 10.3969/j.issn.1007-7294.2016.05.002
- Dong GH, Yao CB, Feng DK, Wang W, Tan Y (2022) Study on drag performance of submarine in density stratified flow. *Shipbuilding of China* 63(3): 11. (in Chinese) DOI: 10.3969/j.issn.1000-4882.2022.03.005
- Faltinsen OM (2006) *Hydrodynamics of high-speed marine vehicles*. Cambridge University Press, Cambridge, New York, 138-140
- Grue J, Friis HA, Palm E, Rusås PO (1997) A method for computing unsteady fully nonlinear interfacial waves. *Journal of Fluid Mechanics* 351: 223-252. DOI: 10.1017/S0022112097007428
- He GH, Liu S, Wang W, Pan YJ (2021) The analysis of the influence of density stratification on the wave resistance of the submersible surface of the near water. *Journal of Harbin Engineering University* 42(8): 1125-1132. (in Chinese) DOI: 10.11990/jheu.202004032
- He GH, Liu S, Zhang ZG, Zhang W, Wang W, Gao Y, Pan YJ (2022) Analysis on the wake of submarine navigating in deeper density layer. *Journal of Harbin Institute of Technology* 54(1): 40-48. (in Chinese) DOI: 10.11918/202008068
- Hu KY, Pan LM, Yu X, Yang ZC, Shi LF (2020) Numerical simulation of moving ellipsoidal wake field in stratified flow with pycnocline. *Proceedings of the 31st National Symposium on Hydrodynamics*, Xiamen, 402-411. (in Chinese) DOI: 10.26914/c.cnkihy.2020.036988
- Huang FL, Cao LS, Wan DC (2020) Numerical simulation of complex flow field in submarine near surface navigation in continuous density stratified flow. *Proceedings of the 31st National Symposium on Hydrodynamics*, Xiamen, 857-870. (in Chinese) DOI: 10.26914/c.cnkihy.2020.037045
- Huang FL, Meng QJ, Cao LS, Wan DC (2022) Wakes and free surface signatures of a generic submarine in the homogeneous and linearly stratified fluid. *Ocean Engineering* 250: 111062. DOI: 10.1016/j.oceaneng.2022.111062
- Landau LD, Lifshitz EM (1959) *Fluid mechanics*. Pergamon Press, Oxford, England, 35-37
- Li SQ, Xiao CR, Cao ZJ (2018) Numerical analysis of wake flow and hydrodynamics for a submarine based on STAR-CCM+. *Chinese Journal of Ship Research* 13(S1): 29-35. (in Chinese) DOI: 10.19693/j.issn.1673-3185.01216
- Liu JF, Mao KX, Zhang XJ, Liang XY, Li Y (2013) The general distribution characteristics of pycnocline of China Sea. *Marine Forecasts* 30(6): 21-27. (in Chinese) DOI: 10.11737/j.issn.1003-0239.2013.06.004
- Liu S, He GH, Wang W, Wang ZK, Luan ZX, Zhang ZG (2020) Resistance and flow field of a submarine in a density stratified fluid. *Ocean Engineering* 217(1): 107934. DOI: 10.1016/j.oceaneng.2020.107934

- Liu S, He GH, Wang W, Gao Y (2021a) Analysis on the wake of a shallow navigation submarine in the density-stratified fluid. *Journal of Harbin Institute of Technology* 53(7): 52-59. (in Chinese) DOI: 10.11918/202005023
- Liu S, He GH, Wang W, Gao Y (2021b) Effect of appendages on hydrodynamic characteristics of submarine in stratified fluid. *Acta Armamentarii* 42(1): 108-117. (in Chinese) DOI: 10.3969/j.issn.1000-1093.2021.01.012
- Liu S, He GH, Wang W, Pan YJ (2021c) Effect of density stratification on wave-making resistance of submarine navigating in deep-water. *Journal of Harbin Engineering University* 42(9): 1373-1379. (in Chinese) DOI: 10.11990/jheu.202005056
- Luo H, Chen K, You YX, Wei G (2007) The numerical simulation of interaction between free surface wake generated by a moving submerged body and stochastic ocean waves. *Journal of Shanghai Jiao Tong University* (9): 1435-1440. (in Chinese) DOI: 10.16183/j.cnki.jsjtu.2007.09.010
- Ma WZ, Li YB, Ding Y, Duan F, Hu KY (2020) Numerical investigation of internal wave and free surface wave induced by the DARPA Suboff moving in a strongly stratified fluid. *Ships and Offshore Structures* 15(6): 587-604. DOI: 10.1080/17445302.2019.1661633
- Wang C, Du W, Li GH, Du P, Zhao S, Li ZY, Chen XP, Hu HB (2022) Numerical simulation of underwater vehicle hydrodynamic characteristics influenced by ocean internal waves. *Chinese Journal of Ship Research* 17(3): 102-111. (in Chinese) DOI: 10.19693/j.issn.1673-3185.02742
- Wei G, Le JC, Dai SQ (2003) Surface effects of internal wave generated by a moving source in a two-layer fluid of finite depth. *Applied Mathematics and Mechanics* 24(9): 13. DOI: 10.3321/j.issn:1000-0887.2003.09.004
- Yeung RW, Nguyen TC (1999) Waves generated by a moving source in a two-layer ocean of finite depth. *Journal of Engineering Mathematics* 35: 85-107. DOI: 10.1023/A:1004399917692
- Yu X, Hu KY (2022) Influence of submarine's acceleration and deceleration on wake spectrum characteristics in stratified flow. *Chinese Journal of Ship Research* 17(3): 67-77, 101. (in Chinese) DOI: 10.19693/j.issn.1673-3185.02490
- Zhang MN, Liu JF, Mao KX, Li Y, Zhang XH (2006) The general distribution characteristics of thermocline of China Sea. *Marine Forecasts* 23(4): 51-58. DOI: 10.3969/j.issn.1003-0239.2006.04.007 (in Chinese)
- Zhao BB, Zhang TY, Li LJ, Wang Z, Duan WY, Hayatdavoodi M (2022) Extension of MCC-FS model to bottom time-varying problems. *The 37th International Workshop on Water Waves and Floating Bodies*, Giardini Naxos, Italy, 190-193